Bioorganic & Medicinal Chemistry Letters 25 (2015) 2634–2638

Contents lists available at ScienceDirect

Bioorganic & Medicinal Chemistry Letters

journal homepage: www.elsevier.com/locate/bmcl

DNA specific fluorescent symmetric dimeric bisbenzimidazoles DBP(*n*): The synthesis, spectral properties, and biological activity

Alexander A. Ivanov [b], Vasiliy S. Koval [c], Olga Yu. Susova [b], Victor I. Salyanov [a], Vladimir A. Oleinikov [c], Andrey A. Stomakhin [a], Natalya A. Shalginskikh [b], Margarita A. Kvasha [d], Olga V. Kirsanova [d], Elizaveta S. Gromova [d], Alexei L. Zhuze [a,*]

[a] *Engelhardt Institute of Molecular Biology, Russian Academy of Sciences, Vavilova St. 32, Moscow 119991, Russia*
[b] *Institute of Carcinogenesis, Blokhin Cancer Research Center, Russian Academy of Medical Sciences, Kashirskoye Shosse 24, Moscow 115478, Russia*
[c] *Shemyakin-Ovchinnikov Institute of Bioorganic Chemistry, Russian Academy of Sciences, ul. Miklukho-Maklaya 16/10, Moscow 117997, Russia*
[d] *Chemistry Department, Moscow State University, Moscow 119991, Russia*

ARTICLE INFO

Article history:
Received 27 February 2015
Revised 24 April 2015
Accepted 25 April 2015
Available online 5 May 2015

Keywords:
Dimeric bisbenzimidazoles
Minor groove binders
DNA topoisomerase-I
DNA methyltransferase
Inhibitors

ABSTRACT

A series of new fluorescent symmetric dimeric bisbenzimidazoles **DBP**(***n***) bearing bisbenzimidazole fragments joined by oligomethylene linkers with a central 1,4-piperazine residue were synthesized. The complex formation of **DBP**(***n***) in the DNA minor groove was demonstrated. The **DBP**(***n***) at micromolar concentrations inhibit in vitro eukaryotic DNA topoisomerase I and prokaryotic DNA methyltransferase (MTase) M.SssI. The **DBP**(***n***) were soluble well in aqueous solutions and could penetrate cell and nuclear membranes and stain DNA in live cells. The **DBP**(***n***) displayed a moderate effect on the reactivation of gene expression.

The design of low molecular weight compounds that can site-specifically recognize DNA sequences is one of the topical tasks of bioorganic chemistry and molecular biology. In future the development of molecular tools specifically binding to the target nucleotide sequences in the genome would make it possible to use them for studying and monitoring the expression of the target genes. In addition, these target-directed compounds are of special interest for pharmacology, since the chemotherapeutic activity of the most currently used anticancer drugs depends on their affinity and selectivity toward DNA. In this context low molecular weight compounds noncovalently interacting with DNA in the minor groove are most promising. To a considerable degree, such minor-groove ligands do not suffer from the drawbacks of routine biologically active compounds derived from alkylating agents and intercalators. In particular, they do not damage DNA or distort its structure, and display only insignificant mutagenic effects. In this work we continued our studies on the design of DNA site-specific ligands derived from Hoechst 33258 (**Ht**).[1] This dye is widely used in cytology as a DNA specific fluorescent probe[2] due to the specific binding to A–T pairs in the DNA minor groove,[3,4] capable of inhibition of the TATA-box binding protein,[5,6] topo-I,[7], topo-II,[8] and DNA helicase,[9] and have radioprotector properties.[10] The **Ht** A–T specificity is determined by the dye backbone composed of two benzimidazole fragments linked in the head-to-tail mode. Upon the DNA interaction each of the benzimidazole fragments forms a bifurcation (three-centered) hydrogen bond with thymine O2- or adenine N3-atoms of two adjacent A–T pairs, thus covering an area of about one and a half base pairs.[4,3] The **Ht** binding is also stabilized by electrostatic and intense Van der Waals interactions with DNA minor groove walls.

With the goal of designing the compounds capable of noncovalent and site-specific binding in the DNA minor groove we synthesized and studied **Ht**-derived dimeric analogues **DB**(***n***) (Fig. 1).[1,11] The bisbenzimidazole fragments of these compounds were joined with oligomethylene linkers of varied lengths ($n = 3, 4, 5, 7, 11$), which made their structures isogeometrical to the structure of the minor groove. Some bidentate ligands capable of recognizing nucleotide sequences with two remote AT pairs were obtained.

The **DB**(***n***) inhibited several DNA dependent enzymes, namely, eukaryotic topo-I,[12] murine Dnmt3a MTase,[13] and human hepatitis C NS3 protein (the helicase activity)[14] at low micromolar concentrations. They proved to be promising florescent dyes penetrable cell and nuclear membranes and effectively staining cell nuclei as

* Corresponding author. Tel.: +7 499 135 9718; fax: +7 499 135 1405.
E-mail address: zhuze@eimb.ru (A.L. Zhuze).

http://dx.doi.org/10.1016/j.bmcl.2015.04.087
0960-894X/

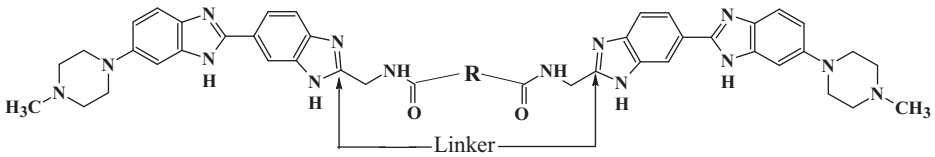

DB(n), **R** = $(CH_2)_n$, where **n** = 1, 2, 3, 5, 7, 9,11

DBP(n), **R** = $(CH_2)_n$-**Pip**-$(CH_2)_n$, where **n** = 1, 2, 3, 4, **Pip** =

Linker length for

DB(5) - *14.8 A* - **DBP(1)** - *14.6 A*; **DB(7)** - *17.8 A* - **DBP(2)** - *17.6 A*;
DB(9) - *20.8 A* - **DBP(3)** - *20.6 A*; **DB(11)** - *23.8 A* - **DBP(4)** - *23.6 A*

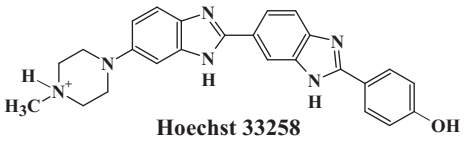

Hoechst 33258

Figure 1. Hoechst 33258, dimeric bisbenzimidazoles **DB**(***n***), **DBP**(***n***) and pairwise comparison of **DB**(**5**,**7**,**9**,**11**) and **DBP**(**1**,**2**,**3**,**4**) linker lengths.

well as providing differential staining of chromosomes.[15] However, due to the tendency to the aggregate formation these compounds were low soluble in aqueous solutions. With the goal of improving the solubility in aqueous solutions and increasing the affinity to DNA complexes we introduced a 1,4-piperazine residue in the oligomethylene linker. We synthesized and studied a series of dimeric bisbenzimidazoles **DBP**(***n***) (*n* = 1–4) (Fig. 1), which are tetracations at neutral pH, unlike **DB**(***n***), which are dications.

The synthesis of dimeric bisbenzimidazoles **DBP**(***n***) is shown in Scheme 1. 1,4-Piperazinalkyldicarboxylic acids (II) were obtained by alkylation of 1,4-piperazine with nitriles of ω-bromoalkylcarboxylic acids followed by the hydrolysis of the resulting dinitriles of 1,4-piperazinodicarboxylic acids with hydrochloric acid. The target bisbenzimidazoles **DBP**(***n***) were prepared by the coupling of monomeric bisbenzimidazole **MB**[1] (Scheme 1) with 1,4-piperazinalkyldicarboxylic acids (II) in the presence of BOP (benzotriazol-1-yloxy)tris(dimethylamino)phosphonium hexafluorophosphate).

Physicochemical studies of **DBP**(***n***)–DNA interactions were performed with the calf thymus DNA (Sigma, United States) using several spectral methods. The absorption spectra were similar for all members of the series (see the Supporting information Fig. S2). At the increased DNA concentrations a hypochromic effect and a small bathochromic effect for the absorption band were observed. This type of changes was also observed for **DB**(***n***)[1] and can evidence the **DBP**(***n***)–DNA complex formation.

Fluorescence spectra of **DBP**(**1**–**4**) were obtained both with and without DNA. In both cases the spectra within the series were also similar. The **DBP**(**1**) fluorescence spectra are shown in Figure S2. The addition of DNA resulted in a shift of the emission band maximum from 468 to 475 nm and an increase in the fluorescence intensity. These data also supported the **DBP**(***n***) complex formation with DNA.

For the localization of **DBP**(***n***) in the complex with DNA we used the CD approach with DNA cholesteric liquid crystal dispersions (CLCD). It was previously shown in[16,17] that the sign of the intensive CD bands of the ligands fixed on the DNA matrix was determined by their orientation toward the long axis of the DNA molecule. A negative band corresponded to the inclination of the ligand chromophore within 54–90°, whereas the positive one, to 0 to 54°. At the angle value of 54° the ligand chromophores were optically inactive. The presence of the positive CD band in the **DBP**(**1**) absorption area (320–335 nm) (Fig. S2c) evidenced that the angle between the ligand chromophore and the DNA long axis was less than 54° and thus supported the **DBP**(**1**) localization in the

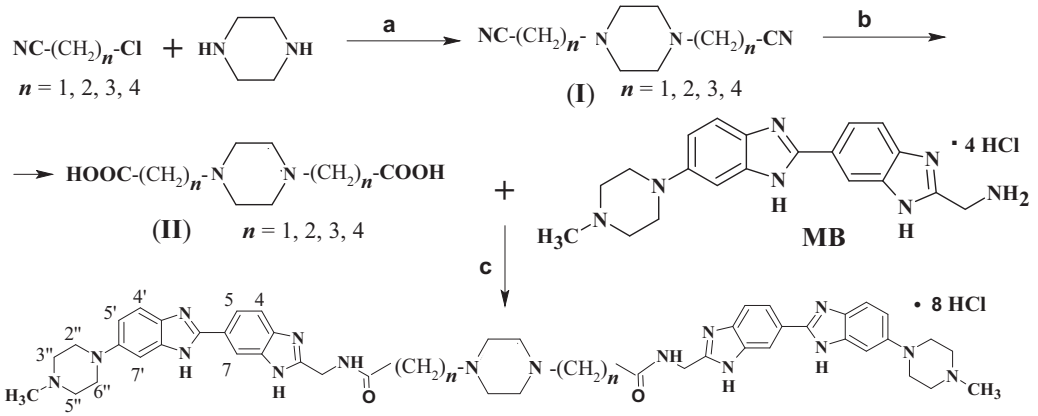

DBP(1) ***n*** **= 1**; **DBP(2)** ***n*** **= 2**; **DBP(3)** ***n*** **= 3**; **DBP(4)** ***n*** **= 4**

Scheme 1. Synthesis of **DBP**(**1**,**2**,**3**,**4**). Reagents and conditions: (a) K_2CO_3, toluene, 110 °C, 21–32%; (b) HCl_{conc}, 100 °C, 2 h, 65–88%; (c) BOP, DIPEA, DMF, 0 °C → room temperature, 12 h, 76–82%. DIPEA – *N*,*N*-Diisopropylethylamine.

DNA groove. Taking into consideration that **DBP**(**1**) is a dimer of **MB** (**Ht** derivative) and, according to the X-ray data, **Ht** is known to bind to DNA in the minor groove,[3,4] we supposed that upon the complex formation **DBP**(**1**) was also located in the DNA minor groove. Similar variations in the CD spectra were observed for **DBP**(**2**–**4**) (spectra are not shown), and this allowed us to conclude that **DBP**(**2**–**4**) are also DNA-specific minor groove ligands.

For the evaluation of dissociation constants (K_d) of **DBP**(***n***)–DNA complexes we studied the fluorescence spectra of the **DBP**(***n***) binding to a 30-bp DNA duplex **A** containing the CpG recognition site of prokaryotic MTase M.SssI (target Cyt residues are underlined):

5'-CTGAATACTACTTG**C**<u>**G**</u>CTCTCTAACCTGAT
3'-GACTTATGATGAAC**G**<u>**C**</u>GAGAGATTGGACTA **A**

The fluorescence of compounds **DBP**(***n***) enhanced upon increasing the DNA duplex concentrations (data not shown). The saturation binding curves, that is, the DNA concentration dependence of the fluorescence intensity at 460 nm, were obtained (Fig. S3). Using the one site hyperbolic binding equation we calculated K_d values (Table 1).

The efficacy of **DBP**(**1**) binding to duplex **A** was nearly the same as for compound **DB**(**11**), for which K_d was 0.39 μM (Cherepanova et al., unpublished data). **DBP**(**2**), **DBP**(**3**) and **DBP**(**4**) bound to duplex **A** even better than **DB**(**11**). Thus we showed the capacity of **DBP**(***n***) to bind to duplex **A** and used these substrates for the studies of the methylation reaction inhibition.

Previously we found and studied the inhibitory properties of **DB**(***n***) toward murine Dnmt3a MTase[13] and received the first data on the demethylation activity of these compounds in normal and tumor cells.[18] However, due the low solubility of **DB**(***n***) in aqueous solutions the stock solutions could be only prepared in dimethylsulfoxide, which was toxic for the cells. An increased solubility due to the introduction of a 1,4-piperazine residue in the oligomethylene linker made it possible **DBP**(***n***) aqueous solutions. The DNA methylation is one of the most intensely studied epigenetic modifications playing an important role for the control of gene expression in eukaryotic cells.[19] Local hypermethylation of promoter gene regions was found in human tumor cells, particularly, in the promotor regions of tumor suppressor genes resulting in their inactivation.[20–22] The DNA methylation status depends on the MTases functioning. This is the reason for an increased interest in the inhibition of the activity of these enzymes.[23]

Inhibitory effects of the **DBP**(***n***) synthesized toward DNA methylation were studied using prokaryotic M.SssI MTase, which, similarly to mammalian MTases, can recognize and methylate DNA CpG sites in positions 5 of the cytosine residues. Duplex **A** labeled at the 5′-end of the upper strand with 6(5)-carboxyfluoresceine (**fA**) was used as a substrate. For the complex formation, duplex **fA** was incubated in the presence of 0–200 μM **DBP**(***n***) for 3 days. The **fA** methylation was visualized by digestion with the methylation-sensitive restriction enzyme R.Hin6I (GCGC recognition site). Nonmethylated molecules were cleaved at the GCGC site to give 14- and 16-membered fragments, whereas methylated molecules were not affected. After the electrophoretic separation in denaturing PAG the methylation degree of duplex **fA** was determined on the basis of fluorescence of the 14-membered product and 30-membered uncleaved oligonucleotide (Fig. 2A). Relative methylation degrees R were calculated using the samples lacking the inhibitor[24]. The IC_{50} values were determined using the function of the *R* value versus **DBP**(***n***) concentrations (Fig. 2B and Table 2).

Table 1
Binding of **DBP**(***n***) to duplex **A**

Compound	**DBP**(**1**)	**DBP**(**2**)	**DBP**(**3**)	**DBP**(**4**)
K_d (μM)	0.37	0.12	0.07	0.07

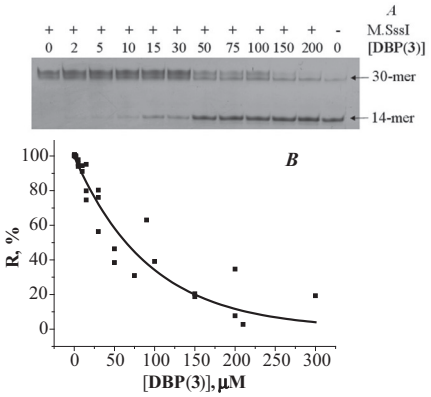

Figure 2. Inhibition of the methylation activity of M.SssI by **DBP**(**3**). (A) Cleavage of **fA** duplex with R.Hin6I endonuclease after its methylation with M.SssI in the presence of 0–200 μM **DBP**(**3**). [**fA**] 300 nM, [*S*-adenosyl-L-methionine] 25 μM, [M.SssI] 2 μM. 20% PAG under denatured conditions (7 M urea) followed by gel imaging on a FUJIFILM FLA-3000 device. (B) The relative methylation degree R of duplex **fA** plotted against the **DBP**(**3**) inhibitor concentration.

Table 2
Inhibition of methylation of **fA** duplex by M.SssI in the presence of **DBP**(***n***)

Compound	**DBP**(**1**)	**DBP**(**2**)	**DBP**(**3**)	**DBP**(**4**)
IC_{50} ± SEM* (μM)	74 ± 11	76 ± 10	64 ± 6.5	63 ± 5

* Mean values of three experiments.

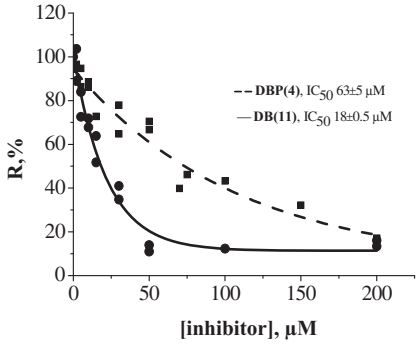

Figure 3. The relative methylation degree R of duplex **fA** by M.SssI plotted against the ●**DB**(**11**) and ■ **DBP**(**4**) inhibitor concentrations.

As is seen in Table 2, all the four **DBP**(***n***) inhibited the M.SssI-mediated methylation of duplex **fA** at micromolar concentrations. No essential differences in the inhibition activities were observed within the series.

We compared inhibitory activities of **DBP**(**4**) and dimeric bisbenzimidazole **DB**(**11**) lacking a piperazine residue (Fig. 1). This pair of compounds was chosen due to approximately the same linker lengths between the bisbenzimidazole blocks (Fig. 1). Compound **DBP**(**4**) was a less effective inhibitor of **fA** methylation than **DB**(**11**), although its IC_{50} remained within the micromolar range (Fig. 3). Despite the lower inhibitory activity of **DBP**(**4**) if compared with the **DB**(***n***) counterpart, the study of **DBP**(***n***) as MTase inhibitors in normal and tumor cells is of a considerable interest.

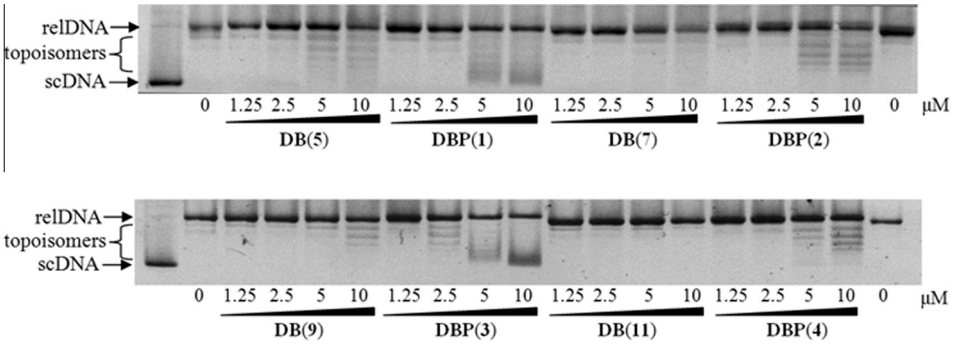

Figure 4. Inhibition of topo-I by **DB**(***n***) and **DBP**(***n***) with the similar linker size at concentrations of 0–10 μM. relDNA, relaxed DNA.

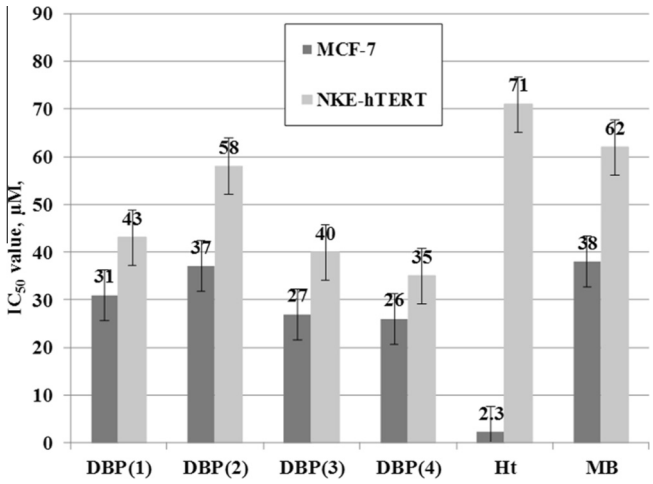

Figure 5. Cytotoxicity of dimeric **DBP**(***n***) and monomeric **Ht** и **MB** bisbenzimidazoles toward MCF-7 and NKE-hTERT cell lines. Cell viability after the 72 h incubation with the compounds under study in the MTT test. IC50 – the concentration of compound yielding 50% of control cell survival.

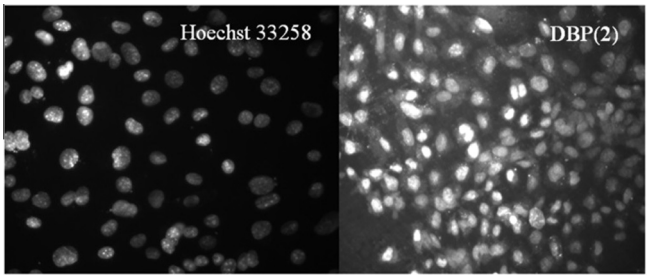

Figure 6. Incorporation of Hoechst 33258 and dimeric bisbenzimidazole **DBP**(**2**) in living mouse fibroblast cells. Excitation of fluorescence at the wavelengths of the UV region.

Topo-I is one of the key enzymes of the cell life. It regulates DNA topology in the processes of transcription, replication, recombination, and repairing. This enzyme relaxes supercoil DNA (scDNA) molecules by inducing single strand breaks followed by the repair of the scDNA covalent integrity by ligation.[25] Currently topo-I is a common target for numerous antitumor agents.[25,26] For the evaluation of dimeric bisbenzimidazoles of the **DBP**(***n***) series as topo-I inhibitors we compared them in pairs with the proper counterparts of the **DB**(***n***) series. We chose the pairs with approximately the same linker length between the bisbenzimidasole fragments (Fig. 1, the linker size is shown with arrows).

The inhibitory properties were tested in vitro in the relaxation reaction of plasmid DNA of eukaryotic topo-I (Topogen, TG1018-2). **DBP**(***n***) and **DB**(***n***) at concentrations of 0–10 μM were incubated for 2 days in aqueous solutions for the formation of linear molecules and then 1 day with plasmid scDNA for the formation of a stable complex. Linear molecules of this type are known to cover the maximum number of DNA base pairs.[27] The capacity of the compounds to inhibit topo-I was estimated visually based on the remained scDNA or its topoisomers after PAGE followed by staining in ethidium bromide (Fig. 4). Compounds **DBP**(**1**) and **DBP**(**2**) at the concentrations of 5 and 10 μM inhibited topo-I more effectively than **DB**(**5**) and **DB**(**7**), respectively. Compound **DBP**(**3**) demonstrated higher inhibitory properties than **DB**(**9**): the same degree of the scDNA relaxation delay was observed at 2.5 μM versus 10 μM, respectively. Thus, **DBP**(**3**) was four times as effective as **DB**(**9**). In another pair, **DPB**(**4**) was markedly more effective than **DB**(**11**): the inhibitory effect of **DPB**(**4**) was seen at a concentration of 5 μM, whereas **DB**(**11**) did not demonstrate the activity even at a concentration of 10 μM. Thus, the compounds of the **DPB**(***n***) series are more effective inhibitors of topo-I.

Cytotoxicity of **DBP**(***n***) was evaluated in the MTT test using human breast tumor MCF-7 cells and human normal kidney epithelial NKE-hTERT cells. The results of the MTT test are shown in Figure 5. All dimeric bisbenzimidazoles **DBP**(***n***) as well as monomeric bisbenzimidazoles **Ht** (Fig. 1) and **MB** (Scheme 1) displayed higher cytotoxicity toward tumor MCF-7 cells than toward normal NKE-hTERT cells. At the same time **DBP**(***n***) were less toxic for tumor MCF-7 cell line than **Ht**.

Penetration of **DBP**(***n***) into cells was studied by fluorescence microscopy. All the **DBP**(***n***) tested were well soluble in aqueous solutions, penetrated cell and nuclear membranes, and stained DNA in living cells (Fig. 6).

Considering that **DBP**(***n***) inhibited the enzymatic activity of MTases as well as topo-I we studied potential biological effects of these compounds on transcription regulation of epigenetically silenced genes. For the analysis we used HeLa-TI population containing the integrated epigenetically repressed avian sarcoma genome with silent green fluorescent protein (GFP).[28–30] The compounds of the **DBP**(***n***) series demonstrated a moderate effect on the reactivation of gene expression if compared with 5-azacytidine (5-AzaC), a DNA methylation inhibitor, and camptothecin, a topo-1 inhibitor, **DBP**(**3**) being the most effective agent of the series (Fig. 7).

To summarize, we have completed the synthesis and DNA binding studies of **DBP**(***n***), a new series of dimeric bisbenzimidazoles. An obvious advantage of these compounds over the previous **DB**(***n***) series is their good solubility in aqueous solutions.

DBP(***n***) can penetrate cell and nuclear membranes of living cells followed by staining cell DNA nuclei, and inhibit in vitro the catalytic activity of prokaryotic M.SssI MTase and eukaryotic topo-I at micromolar concentrations. They proved to be more effective

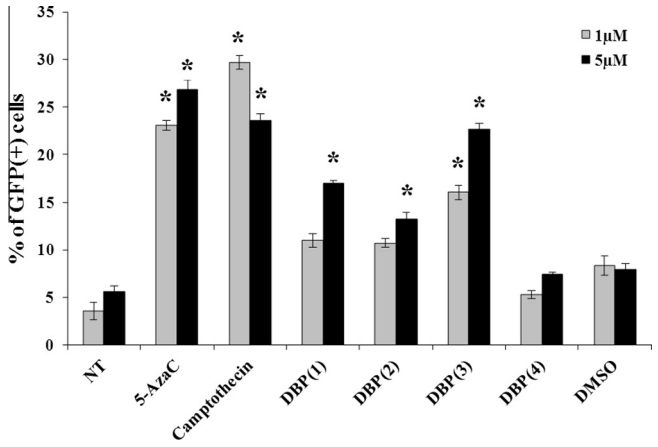

Figure 7. Effect of **DBP**(***n***) on gene expression. Percentage of green (GFP positive) cells (% of GFP(+) cells) was measured by FACS analysis (flow cytometry) 48 h after the drug treatment started. NT – not treated. Statistically significant results with *p*-value <0.01 are marked with asterisks.

inhibitors of topo-I than **DB**(***n***). Dimeric bisbenzimidazoles **DBP**(***n***) were shown to reactivate the expression of epigenetically silenced genes. These results allowed us to treat **DBP**(***n***) as promising agents, inhibitors of MTases, for antitumor therapy. Also, due to the low cytotoxicity **DBP**(***n***) can be used for the design of DNA specific ligands for protection of cell DNA (Veiko co-workers, unpublished data). Further biological studies of **DBP**(***n***) are in progress and the results will be reported elsewhere.

Acknowledgments

This work was supported by the Program of the Presidium of the Russian Academy of Sciences 'Molecular and Cell Biology' and the Russian Foundation for Basic Research (Projects No. 14-04-00388, 12-04-01229, and 13-04-00727). The authors are grateful to Dr. Richard A. Katz and his coworkers for providing the HeLa TI cell line and Dr. Katerina Gurova for the NKE-hTERT cell line.

Supplementary data

Supplementary data associated with this article can be found, in the online version, at http://dx.doi.org/10.1016/j.bmcl.2015.04.087.

References and notes

1. Ivanov, A. A.; Salyanov, V. I.; Streltsov, S. A.; Cherepanova, N. A.; Gromova, E. S.; Zhuze, A. L. *Bioorg. Chem. (Moscow)* **2011**, *37*, 472.
2. Latt, S. A. *Annu. Rev. Biophys. Bioeng.* **1976**, *5*, 1.
3. Teng, M.-K.; Usman, N.; Frederick, C. A.; Wang, A. H.-J. *Nucleic Acids Res.* **1988**, *16*, 2671.
4. Vega, M. C.; Saez, I. G.; Aymami, J.; Eritja, R.; Van der Marel, G. A.; Van Boom, J. H.; Rich, A.; Coll, M. *Eur. J. Biochem.* **1994**, *222*, 721.
5. Chiang, S.-Y.; Welch, J.; Rauscher, F., III; Beerman, T. *Biochemistry* **1994**, *33*, 7033.
6. Chiang, S.-Y.; Welch, J. J.; Frank, R. J., III; Beerman, T. A. *J. Biol. Chem.* **1996**, *271*, 23999.
7. Chen, A. Y.; Yu, C.; Gatto, B.; Liu, L. F. *Proc. Natl. Acad. Sci. U.S.A.* **1993**, *90*, 8131.
8. Woynarowski, J. M.; McHugh, M.; Sigmund, R. D.; Beerman, T. A. *Mol. Pharmacol.* **1989**, *35*, 177.
9. Soderlind, K.-J.; Gorodetsky, B.; Singh, A. K.; Bachur, N. R.; Miller, G. G.; Lown, J. W. *Anti-Cancer Drug Des.* **1999**, *14*, 19.
10. Lyubimova, N. V.; Coutlas, P. G.; Yuen, K.; Martin, R. F. *Br. J. Radiol.* **2001**, *74*, 77.
11. Ivanov, A. A.; Streltsov, S. A.; Prikazchikova, T. A.; Gottikh, M. B.; Zhuze, A. L. *Bioorg. Chem. (Moscow)* **2008**, *34*, 261.
12. Susova, O. Yu.; Ivanov, A. A.; Ruiz, S. S.; Morales; Lesovaya, E. A.; Gromyko, A. V.; Streltsov, S. A.; Zhuze, A. L. *Biochem. (Moscow)* **2010**, *75*, 695.
13. Cherepanova, N. A.; Ivanov, A. A.; Maltseva, D. V.; Minero, A. S.; Gromyko, A. V.; Streltsov, S. A.; Zhuze, A. L.; Gromova, E. S. *J. Enzyme Inhib. Med. Chem.* **2011**, *26*, 295.
14. Tunitskaya, V. L.; Mukovnya, A. V.; Ivanov, A. A.; Gromyko, A. V.; Ivanov, A. V.; Streltsov, S. A.; Zhuze, A. L.; Kochetkov, S. N. *Bioorg. Med. Chem. Lett.* **2011**, *21*, 5331.
15. Popov, K. V.; Egorova, E. I.; Ivanov, A. A.; Gromyko, A. V.; Zhuze, A. L.; Bolsheva, N. L.; Yurkevitch, O. Yu.; Muravenko, O. V.; Zelenin, A. V. *Biochem. (Moscow) Suppl. Ser. A: Mem. Cell Biol.* **2008**, *2*, 203.
16. Norden, B. *Appl. Spectrosc. Rev.* **1978**, *14*, 157.
17. Yevdokimov, Yu. M.; Skuridin, S. G.; Lortkipanidze, G. B. *Liq. Cryst.* **1992**, *12*, 1.
18. Pommier, Y. *Nat. Rev. Cancer* **2006**, *6*, 789.
19. Bird, A. *Genes Dev* **2002**, *16*, 6.
20. Jones, P. A.; Baylin, S. B. *Nat. Rev. Genet.* **2002**, *3*, 415.
21. Baylin, S. B.; Esteller, M.; Rountree, M. R.; Bachman, K. E.; Schuebel, K.; Herman, J. G. *Hum. Mol. Genet.* **2001**, *10*, 687.
22. Jones, P. A.; Baylin, S. B. *Cell* **2007**, *128*, 683.
23. Gowher, H.; Jeltsch, A. *Cancer Biol. Ther.* **2004**, *1062*, 3.
24. Darii, M. V.; Rakhimova, A. R.; Tashlitsky, V. N.; Kostyuk, S. V.; Veiko, N. N.; Ivanov, A. A.; Zhuze, A. L.; Gromova, E. S. *Mol. Biol. (Moscow)* **2013**, *47*, 259.
25. Li, T.-K.; Liu, L. F. *Annu. Rev. Pharmacol. Toxicol.* **2001**, *41*, 53.
26. Pommier, Y. *ACS Chem. Biol.* **2013**, *8*, 82.
27. Streltsov, S. A.; Gromyko, A. V.; Oleinikov, V. A.; Zhuze, A. L. *J. Biomol. Struct. Dyn.* **2006**, *24*, 285.
28. Katz, R. A.; Jack-Scott, E.; Narezkina, A.; Palagin, I.; Boimel, P.; Kulkosky, J.; Nicolas, E.; Greger, J. G.; Skalka, A. M. *J. Virol.* **2007**, *81*, 2592.
29. Poleshko, A.; Einarson, M. B.; Shalginskikh, N.; Zhang, R.; Adams, P. D.; Skalka, A. M.; Katz, R. A. *J. Biol. Chem.* **2010**, *285*, 422.
30. Shalginskikh, N.; Poleshko, A.; Skalka, A. M.; Katz, R. A. *J. Virol.* **2013**, *87*, 2137.